Materials Research, Vol. 11, No. 3, 325-333, 2008

Molecular Mechanics Applied to Single-Walled Carbon Nanotubes

Antonio Ferreira Ávila*, Guilherme Silveira Rachid Lacerda

Mechanics of Composites and Nano-Structured Materials Laboratory,
Department of Mechanical Engineering, Universidade Federal de Minas Gerais,
Av. Antonio Carlos, 6627, 31270-901 Belo Horizonte - MG, Brazil

Received: December 10, 2007; Revised: March 17, 2008

Single-walled carbon nanotubes, with stiffness of 1.0 TPa and strength of 60 GPa, are a natural choice for high strength materials. A problem, however, arises when experimental data are compiled. The large variability of experimental data leads to the development of numerical models denominated molecular mechanics, which is a "symbiotic" association of molecular dynamics and solid mechanics. This paper deals with molecular mechanics simulations of single-walled carbon nanotubes. To be able to evaluate the molecular mechanics model, the three major carbon nanotube configurations (armchair, zigzag and chiral) were simulated. It was proven that the carbon nanotube configuration has influence on stiffness. By varying the radius, hence the curvature, the Young's modulus changed from 0.95 TPa to 5.5 TPa, and the Poisson's ratio ranged from 0.15 to 0.29. The numerical simulations were in good agreement with those presented in the literature.

Keywords: *single-walled carbon nanotubes, molecular mechanics, numerical simulation, mechanical properties*

1. Introduction

Carbon nanotubes[1], since their discovery in 1991, have attracted much interest due to their ability of sustaining large deformations, their elevated stiffness and possible high strength. Their capabilities have been observed experimentally and verified by numerical simulations, i.e. molecular dynamics[2-4], atomistic simulations[5-6] and nano-mechanics modeling[7-9]. Although carbon nanotubes have tremendous potential applications in a large variety of usages, e.g. aerospace industry, medical and electronic devices, there is no consensus about their exact mechanical properties. The experiments performed up to now have presented large variability due to the inherent complexity of manipulating these materials. Furthermore, the traditional molecular dynamics (MD) simulations are limited and computationally expensive.

In this paper, the concept of molecular structural mechanics[9,10] is associated to the three-dimensional finite element model and later on employed to predict the Single-Walled Carbon Nanotubes (SWNTs) stiffness. Numerical simulations considering the three main configurations (armchair, zigzag and chiral) are performed. A parametric study on wall thickness, diameter and chirality effects on stiffness is also performed.

2. Literature Review

According to Saito et al.[11], carbon nanotube is a honeycomb lattice rolled into a cylinder. Carbon nanotubes have been the center of many researches due to their dimensions and remarkable electromechanical properties. In general, a carbon nanotube diameter is of nanometer size and its length can be more than 1 μm. As mentioned by Saito and his colleagues, nanotube diameter is much smaller than most advanced semiconductors devices developed so far. Moreover, consistent with Kalamkarov et al.[12], SWNT has predicted specific strength around 600 times larger than steel.

Another important issue of carbon nanotubes is their remarkable thermal and electrical properties. Carbon Nanotubes (CNTs) are thermally stable up to 2800 °C (in vacuum), reveal a thermal conductivity about twice as high as diamond, and may exhibit a capacity to carry electric current a thousand times better than copper wires. With such promising properties, CNTs are natural candidates for reinforcement of advanced composites. Nevertheless, variability from experimental data obtained from CNTs is a problem.

As stated by Natsuki et al.[13], experimental methods for measuring the mechanical properties of CNTs are mainly based on transmission electron microscopy (TEM) and atomic force microscopy (AFM). According to Natsuki et al.[13], by measuring thermal vibration using TEM, Treacy et al obtained a Young modulus of 1.8 ± 0.9 TPa. A different result, also reported by Natsuki et al.[13], was obtained by Wong and his colleagues. The much lower Young's modulus (1.28 ± 0.59 TPa) value reported by Wong can be attributed to the measuring technique. Wong's research group employed the AFM tip to bend anchored multi-walled nanotubes (MWNTs). After measuring the MWNT deflection, Wang calculated the Young's modulus using the continuum mechanics approach. However, by applying this technique, Wong was not able to identify the nanotube diameter influence on stiffness. Furthermore, the MWNTs anchored/clamping condition was also a problem, as the researchers were not able to constrain all degrees-of-freedom as required. Another set of experiments in MWNT was performed by Yu et al.[14]. Yu's experiments lead to Young's modulus ranging from 0.27 to 0.95 TPa. They also reported tensile strength values from 11 to 63 GPa. Notice that Yu's stiffness peak value was half of Treacy's results, and it was still considerably lower than Wong's data. As it can be observed, there is a large discrepancy among the results reported. This phenomenon can be explained by the differences on measuring techniques employed.

The results obtained for single-walled carbon nanotubes follow the same pattern, in other words, a large variability among different sets of experimental data. Krishnan et al.[15] developed a study on SWNT using the TEM technique. The SWNT had a diameter range

*e-mail: aavila@netuno.lcc.ufmg.br

of 1.0-1.5 nm, and the elastic modulus measured was 1.30 ± 0.4 TPa. Yu et al.[14] also obtained the mechanical responses of SWNT bundles under tensile loading. The values of elastic moduli ranged from 0.32 to 1.47 TPa, while Yu's tensile strength measured was between 13 and 53 GPa. It is important to mention that the experimental data discussed up to now were obtained at room temperature. Lourie and Wagner[16] obtained the axial Young's modulus for a wide range of temperatures by employing micro-Raman spectroscopy to nanotubes embedded in the epoxy matrix. To do so, they had to induce a compressive deformation by cooling the nanotubes-epoxy samples. At low temperature, ≈ 80 K, Lourie and Wagner[16] obtained a 3.0 TPa axial Young's modulus for SWNT with an average radius of 0.7 nm, and 2.4 TPa for MWNTs with an average radius of 5-10 nm. Xiao et al.[17], however, reported for SWNT a tensile Young's modulus ranging from 0.27 to 3.6 TPa, while the ultimate strength varied from 11 to 200 GPa. Given the variability of results, Xiao et al.[17] concluded that CNTs elastic properties are highly dependent on its structure.

Due to the complexity in experimental characterization of nanotubes, computer simulation has been looked upon as a powerful tool for modeling nanotubes properties. The fundamental relations governing the geometry of CNTs were described by Dresselhaus et al.[18]. They developed mathematical expressions linking the graphene sheet geometry and the honeycomb-like design to the carbon nanotubes three main configurations (chiral, zigzag and armchair). By doing this, they opened the possibility to computer simulations of CNTs.

For Xiao et al.[17], the large majority of numerical and analytical approaches can be classified into two categories: the "bottom up" approach based on quantum/molecular mechanics including the classical molecular dynamics (MD), and the "top down" based on continuum mechanics. A third category, however, can be established; it is called multi-scale methods, where the continuum mechanics models are coupled to MD expressions.

Wang et al.[19] reported that MD formulations were probably the most popular methods currently employed for nano-scale analysis, due to their accuracy and the large number of interatomic potential functions for a large variety of materials. However, a critical issue on MD simulations remains, i.e. temperature. The temperature induces a high frequency molecular thermal vibration (on scale of 10^{15} Hz) and this vibration makes difficult to estimate strains, even worst, it limits the deformation calculations to pico- or nano-seconds.

Liu et al.[20] mentioned that nanoscale materials are, in general, used in association to other components that are much larger, and have different response times, thus operating at different time and length scales. Due to these limitations, Liu et al.[20] suggested that hybrid models must be design in a micron scale. Micron size models, however, are composed of billions of atoms, which is still too large for MD simulations, even for large computers. Hence, there is a need to develop multi-scale approaches for this class of problems. Li and Chou[21] defined the multi-scale modeling technique as a combination of the atomistic molecular structural mechanics approach and the continuum finite element method[22]. This approach was also implemented by Meo and Rossi[23], where the elements selected were non-linear elastic and linear elastic torsional springs. As mentioned by them, the non-linear elastic spring element was applied due to the lack of information about the sectional properties of carbon-carbon bond. Furthermore, the torsional spring element was used to overcome problems with bond angles bending. They were able to simulate the three main single-walled carbon nanotubes configurations (armchair, zigzag and chiral) and graphene sheets with accuracy. The SWNTs geometric description of Meo and Rossi's model was based on the equations proposed by Koloczek et al.[24]. This approach saved considerable computational efforts during the mesh generation. Their predictions for the graphene sheets Young's modulus were in good agreement with the ones published in literature, i.e. ≈1.03 TPa. The drawback of Meo and Rossi's model is that they were limited to uniaxial tensile problems.

To overcome this problem, Sun and Zhao[25] applied two different element types. The first one was a chemical bond element that represented the intra-molecular potential energy of stretching, bending and torsional conditions. This element was based on a two-node elastic rod element with an elastic joint in each end. The second element was a Lennard-Jones non-linear spring element that took in consideration the inter-molecular potential energy. By modifying the Morse potential function, they were able to model the C-C chemical bond breakage. In sum, they were able to model stiffness and strength simultaneously. However, the data obtained, 0.4 TPa for stiffness and between 77-101 GPa for strength, were below the usual results published in literature. A possible explanation for such behavior can be the excess of compliance introduced during the stiffness matrix derivation. This hypothesis is corroborated by Pantano et al.[26], who related the bending stiffness to the carbon nanotube mean radius and its total wall thickness. Note that for Sun and Zhao[25], the tensile stiffness was practically constant with the increase of the nanotube diameter.

The work developed by Huang et al.[27] gave a step forward by defining the system total energy based on the atomic nucleons locations. However, by considering only stretching and bending, their results were similar to the ones reported by Sun and Zhao[25]. Tserpes and Papanikos[10], however, went further as they employed beam elements in a three-dimensional (3D) space where stretching, bending, out-of-plane torsion, dihedral angle torsion and Van der Waals interactions were considered. This model brought about results with good agreement with the literature and with minimal computational efforts.

The numerical simulations presented are encouraging. Researches, however, are still seeking a more efficient computational modeling for predicting nano-materials properties.

3. Molecular Mechanics Modeling

Dresselhaus et al.[18] described SWNTs in terms of the tube diameter (d) and its chiral angle (θ). The chiral vector (C_h) was defined in terms of the graphene sheet lattice translation integer indices (n,m) and the unit vectors (a_1,a_2) represented in Figure 1, and it is defined as follows:

$$\vec{C}_h = n\vec{a}_1 + m\vec{a}_2 \quad (1)$$

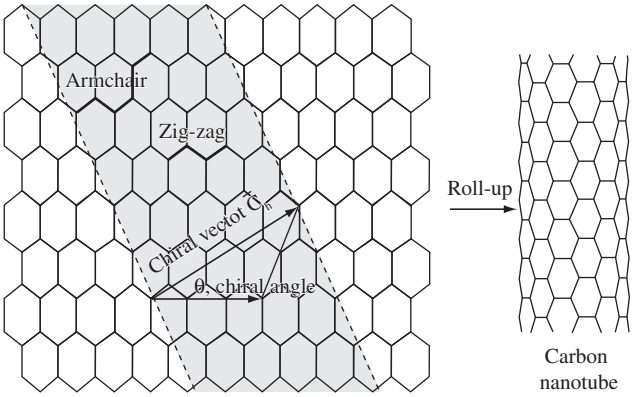

Figure 1. Chiral angle and vector representation adapted from reference 10.

where the unit vectors in (x,y) coordinates are defined as:

$$\vec{a}_1 = \left(\frac{\sqrt{3}}{2}, \frac{1}{2}\right)a \quad \vec{a}_2 = \left(\frac{\sqrt{(3)}}{2}, \frac{1}{2}\right)a \tag{2}$$

the length of the unit vector a is defined as 2.46 angstroms, or 1.73 times the carbon-carbon distance (1.421 angstroms). The nanotube circumference (p) was defined by:

$$p = |c_h| = a\sqrt{n^2 + m^2 + nm} \tag{3}$$

from simple geometry, it is possible to obtain the nanotube diameter (d) as:

$$d = \frac{p}{\pi} = \frac{\sqrt{n^2 + m^2 nm}}{\pi}a \tag{4}$$

and the chiral angle (θ), between 0 and π/6 rad, was described by Dresselhaus et al.[18]

$$\sin\theta = \frac{\sqrt{3}m}{2\sqrt{n^2 + nm + m^2}} \quad \cos\theta = \frac{2n + m}{2\sqrt{n^2 + nm + m^2}} \tag{5}$$

The three main SWNTs configurations described by Kalamkarov et al.[12] are represented in Figure 2. Notice that each configuration has its own cap distinct formation. However, as the aspect ratio (length/diameter) is in general large, it is possible to discard the cap effect without loss of generality.

In the molecular structural mechanics approach, a single-walled carbon nanotube is simulated as a space frame structure, with the covalent bonds and the carbon atoms as connecting beams and joint nodes, respectively. If the beam elements simulating the covalent bonds are assumed to be of round section, then only three stiffness parameters are required to be defined for deformation analysis. These parameters are: the tensile resistance (EA), the flexural rigidity (EI), and the torsional stiffness (GJ).

Li and Chou[21] based their model on the energy equivalence between local potential energies in computational chemistry and elemental strain energies in structural mechanics. By applying this approach, they established a direct relationship between the structural mechanics parameters and the molecular mechanics force field constants. These parameters are mathematically represented by:

$$\frac{EA}{L} = k_r \quad \frac{EI}{L} = k_\theta \quad \frac{GJ}{L} = k_\tau \tag{6}$$

where L denotes the bond length, and k_r, k_θ and k_τ are the force field constants in molecular mechanics. By assuming a circular beam cross section with diameter d, and setting the area, moment of inertia and polar moment of inertia as $A = \pi d^2/4$, $I = \pi d^4/64$ and $J = \pi d^4/32$, Tserpes and Papanikos[10] obtained the following expressions:

$$d = 4\sqrt{\frac{k_\theta}{k_r}} \quad E = \frac{k_r^2 L}{4\pi k_\theta^2} \quad G = \frac{k_r^2 k_\tau L}{8\pi k_\theta^2} \tag{7}$$

As an illustrative example, Figure 3 shows the equivalence of molecular mechanics and sructural mechanics for covalent and non-covalent interactions between carbon atoms. Notice that covalent interactions can be "translated" into molecular mechanics either as tension, bending or torsion. It all depends on atoms positions. The non-covalent interactions, i.e. Van der Wall's interactions, are equivalent to a non-linear spring condition.

According to Ávila and Lacerda[28], the carbon nanotubes stiffness can be predicted following the molecular mechanics approach associated to the concept of representative volume element (RVE). Tamma and Ávila[29] defined the RVE as the material smallest part which retains the overall material properties. When carbon nanotubes are examined, the concept of RVE has to be rearranged so that interactions between the carbon-carbon bonds and the exterior are taken into consideration. Ávila and Lacerda[30] successfully rearranged the RVE concept by applying boundary conditions constraints at atomic level. A similar investigation was applied by Odegard et al.[31] for carbon nanotubes dispersed into a polymeric matrix. In their case, the atomic interactions polymer-carbon nanotubes were modeled by the equivalent truss model, which is similar to the model presented by Ávila and Lacerda[30].

3. Numerical Simulations and Data Analysis

The carbon-carbon bonds are simulated by a beam element with six degrees-of-freedom at each node: translations in nodal x, y, z and rotations about the nodal x, y, z. The beam length was assumed to be equal to 0.1421 nm as suggested by Tserpes and Papanikos[10]. This type of element is capable of uniaxial tension or compression along with torsional and bending deformations. To be able to generate each group of SWNTs (armchair, zigzag and chiral), a macro subroutine was developed and implemented into ANSYS V.10, a commercial finite element code. In the present model, the k_ρ, k_θ and k_τ constants are from Li and Chou[21], and their values are 6.52×10^{-7} N nm rad^{-1}, 8.76×10^{-10} N nm rad^{-2} and 2.78×10^{-10} N nm rad^{-2}, respectively. Figure 4 shows the model mesh for each SWNTs group, and it also indicates the boundary conditions applied. As described by Ávila and Lacerda[30], the representative volume element (RVE) assumes different formats due to the SWNTs configurations. To be more specific: the (4,2) chiral configuration was represented by 112 atoms and 162 C-C bonds, while for the (17,9) chiral format the number of atoms and C-C bonds were 623 and 908, respectively. These changes are the main reason for differences on the RVE total length. Table 1 summarizes the size of the molecular mechanics models for each nanotube simulated.

The research community agrees that nanotube wall thickness has direct effect on stiffness of SWNTs. Thus, to be able to exam the molecular mechanics model accuracy, a series of numerical simulations were performed. For validation purposes, different data from three distinct approaches (MD, continuum and molecular mechanics) were selected. The molecular dynamic (MD) model applied by Yakobson et al.[32] was one of them. Another molecular dynamic approach called tight binding MD described by Hernandez et al.[33] was also selected as benchmark. The continuum shell modeling[26] and the equivalent continuum modeling[31] were chosen as the third and fourth benchmark models, respectively. The fifth benchmark model[34] was based on strain energy theory, which brings some similarities

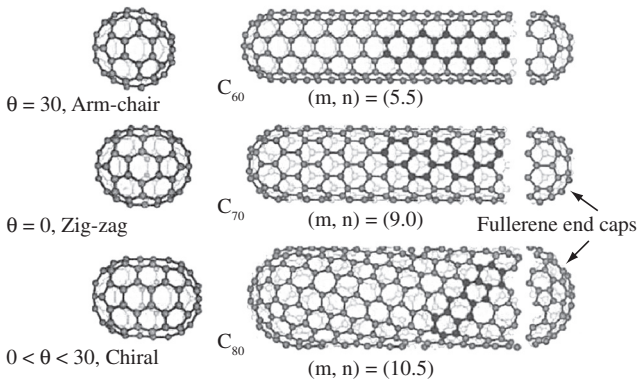

Figure 2. SWNT configurations and their respective caps adapted from reference 12.

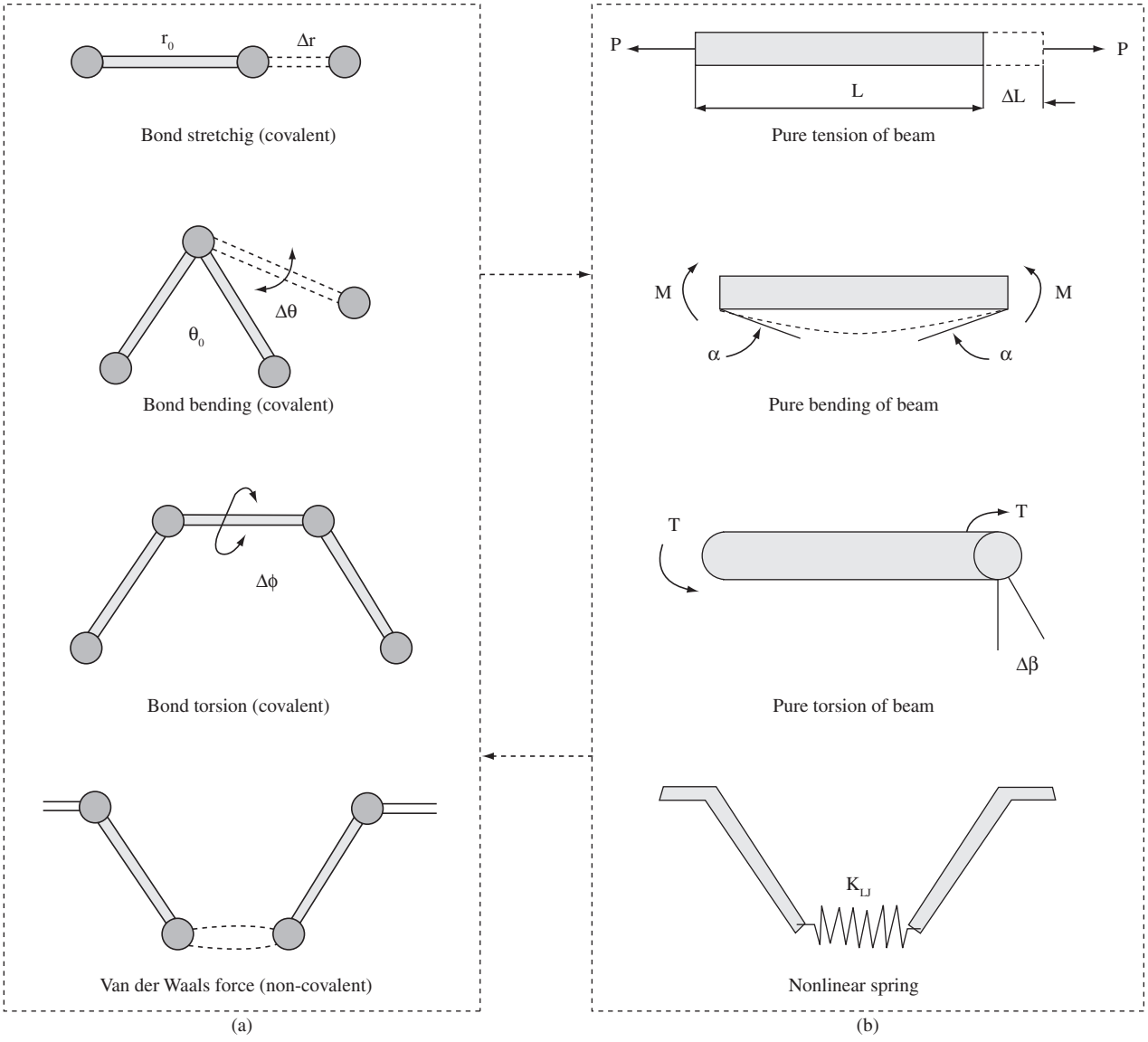

Figure 3. Equivalence between molecular and structural mechanics. a) molecular mechanics; and b) structural mechanics adapted from reference 10.

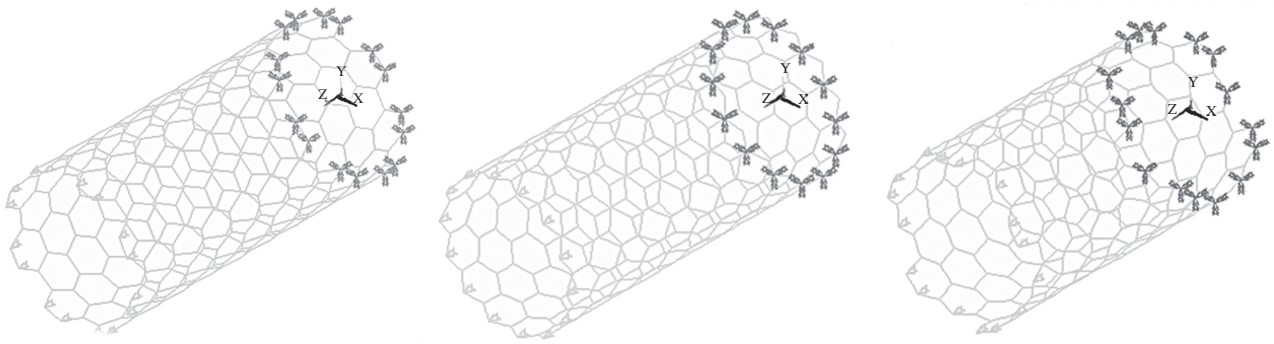

(a) (b) (c)

Figure 4. SWNT mesh and imposed boundary conditions. a) (8,8) Armchair, b) (14,0) zigzag, and c) (11,5) Chiral.

to Pantano's[26] and Odergard's[31] models. Li and Chou[21], Tserpes and Papanikos[10] and Ávila and Lacerda[30] with slight differences, mostly on boundary conditions, applied the molecular mechanics approach to SWNTs and/or MWNTs modeling. Therefore, they were also selected as benchmarks. Three groups of SWNTs were investigated, i.e. armchair (8,8), zigzag (14,0) and chiral (11,5). Table 2 reviews all data obtained and the ones from the benchmark researches.

There is no doubt that carbon nanotube wall thickness has influence on the overall stiffness. When the present model is compared against the three major groups of mathematical modeling (molecular dynamics, continuum mechanics and molecular mechanics) some conclusions can be drawn. The lower and upper bounds of the molecular dynamics predictions are obtained with chiral configuration. The upper bound difference (28.76%) can be explained when the tight binding model is analyzed. Hernandez et al.[33] did not consider the "atoms rotations", in other words, for them stiffness was calculated taking the nanotube strain energy regardless of the chiral angle. The molecular dynamics simulations performed by Yakobson et al.[32] lead to the lower bound difference (10.84%). Note that Yakobson and his collaborators considered the nanotube behavior beyond the nonlinear instability, in other words, they included in their MD simulation the buckling effect. As a consequence, their model was capable to identify with more accuracy the shell energy strain. It is important to recall that carbon nanotubes are essentially long shell columns.

The continuum mechanics based models appear to be more accurate, as the lower and upper bounds range from 1.14 to 10.84%. The models presented by Pantano et al.[26], Odergard et al.[31] and Lu[34] share some similar conditions and dissimilarities. To be more specific, in all three models the stiffness was using the traditional second derivative of the strain energy density with respect to the axial strain. Lu's model, however, has a weakness; the empirical force-constant model employed is insensible to the chiral angle atoms rotation. When complex geometries and deformations are analyzed, the model developed by Odergard and his colleagues requires numerical tools to calculate the continuum parameters. Once the properties of the equivalent-continuum model have been established, the mechanical behavior can be predicted by traditional continuum mechanics. The model created by Pantano et al.[26] uses shell elements associated to the continuum mechanics approach. Shell elements, however, can suffer from interlocking shear problems. To avoid this problem, Odergard et al.[31] employed trust elements in their model. By employing this approach, they were able to reduce the number of degrees-of-freedom and consequently increase the number of atoms in their model. In both cases, the models are in good agreement with experimental and molecular mechanics simulations. The models based on molecular mechanics approach provided the smallest differences between proposed model and the three benchmark models (Li and Chou[21], Ávila and Lacerda[30], Tserpes and Papanikos[10]). Again the largest difference was noticed on chiral condition. This can be due to boundary conditions imposition.

Another important conclusion is that thicker walls guided to smaller Young's modulus. Such hypothesis can be corroborated by

Table 1. Characteristics of molecular mechanics models.

	Chirality (n,m)	Total length (nm)	Number of atoms	Number of elements
Armchair	(3,3)	2.3382	120	174
	(5,5)	2.3382	200	290
	(8,8)	2.3382	320	464
	(11,11)	2.3382	440	638
	(13,13)	2.3382	520	754
Zigzag	(5,0)	2.4157	120	175
	(9,0)	2.4157	216	315
	(14,0)	2.4157	336	490
	(19,0)	2.4157	456	665
	(23,0)	2.4157	552	805
Chiral	(4,2)	2.1854	112	162
	(6,4)	1.8130	152	218
	(11,5)	2.0123	268	386
	(14,8)	2.7255	496	722
	(17,9)	2.8986	623	908

Table 2. Comparative study on wall thickness effect on stiffness (Young's modulus – E).

Reference	Wall thickness (nm)	E (TPa)	Present model		
			(8,8)	(14,0)	(11,5)
Yakobson et al.[32]	0.066	5.5	5.282	5.298	4.962
Hernandez et al.[33]	0.34	1.24	1.025	1.028	0.963
Pantano et al.[26]	0.075	4.84	4.648	4.662	4.367
Lu[34]	0.34	0.974	1.025	1.028	0.963
Odegard et al.[31]	0.69	0.496	0.505	0.507	0.475
Li and Chou†	0.34	1.01	1.025	1.028	0.963
Tserpes and Papanikos[10]†	0.147	2.395	2.377	2.385	2.423
Ávila and Lacerda[28]†	0.34	1.005	1.025	1.028	0.963

†young's modulus (E) is the mean value of these author's predictions.

Odergard et al.[31] that, based on equivalent-continuum model, stated that Young's modulus is inversely proportional to SWNTs cross sectional area. Additionally, Li and Chou[21] attributed the variation among the three configurations to small differences on radii. Tserpes and Papanikos[10], however, also called the attention to the chirality effect. According to them, the diameter effect is more evident on armchair and zigzag configurations, while the chiral form is less affected. Notice that as the nanotube diameter becomes smaller than 1 nm the curvature effect is more evident. Furthermore, as demonstrated by Figure 5, as the nanotube diameter increases, the Young's modulus has an asymptotic behavior which leads to stiffness values close to the graphene sheet. A small nanotube diameter leads to large curvature and distortion of the carbon–carbon (C-C) bonds. This phenomenon brings as a consequence a large elongation (Δh) of the nanotube. As the diameter increases, the curvature effect diminishes and the SWNTs Young's moduli approach the one from the graphene sheet (1.1 TPa) where no curvature effect is present. This is particularly true when the SWNT wall thickness reaches 0.34 nm. As the SWNT is modeled as a three-dimensional tubular structure, the Poisson effect is an important issue.

The classical theory of elasticity[36] defines the Poisson ratio as

$$\nu_{CNT} = -\frac{\varepsilon_{radial}}{\varepsilon_{acial}} = -\frac{\Delta R / R_0}{\Delta H / H_0} \quad (8)$$

where ε_{radial} is the radial strain, ε_{axial} represents the axial strain, ΔH defines the axial displacement imposed to the nanotube, and ΔR is the radial displacement measured. Finally, R_0 and H_0 are the nanotube radius and length, respectively. Figure 6 represents the Poisson's ratio as a function of the nanotube radius. As it can be observed, in all configurations (armchair, zigzag and chiral), the Poisson ratio seems to seek a asymptotic value as the radius gets larger.

The Poisson ratio values obtained vary between 0.28 and 0.36 for armchair, 0.15 and 0.31 for zigzag, while for the chiral configuration the values are between 0.22 and 0.66. The results reported by Salvetat-Delmont and Rubio[37] for nanotubes with diameter larger than 1 nm are between 0.16, 0.19 and 0.18, for armchair, zigzag and chiral, respectively. The difference between the present model and the results supplied by Salvetat-Delmont and Rubio[37] can be attributed to their model uncertainties and the boundary conditions applied. They also mentioned that their results can have an off-set of at least ±10%. When the results are compared against the MD simulations performed by Xiao et al.[17], all three configurations are in good agreement for larger radii. Lu[34] reported Poisson values between 0.26 and 0.32 for diameters larger than 1 nm. Sun and Zhao[25], however, applying the finite element approach in a armchair configuration for 0.8 nm diameter, obtained a 0.35 Poisson ratio, while a nanotube with 2.8 nm diameter lead to a 0.31 Poisson ratio. Notice that for this case, the present model is in good agreement with those results reported by Sun and Zhao.

Natsuki et al.[13] also calculated the Poisson ratio of single-walled carbon nanotubes. Their model was based on analytical model using a three-dimensional grid associated to springs. They reported, for the armchair configuration, values between 0.27-0.29 when the nanotube diameter varied between 0.5-2.5 nm. For the zigzag configuration, the Natsuki's results varied from 0.27 to 0.33 for the same range of diameter. No values for the chiral configuration were reported. A comparison between the present model and the Natsuki's lead to the same conclusion, the results seems to be in good agreement.

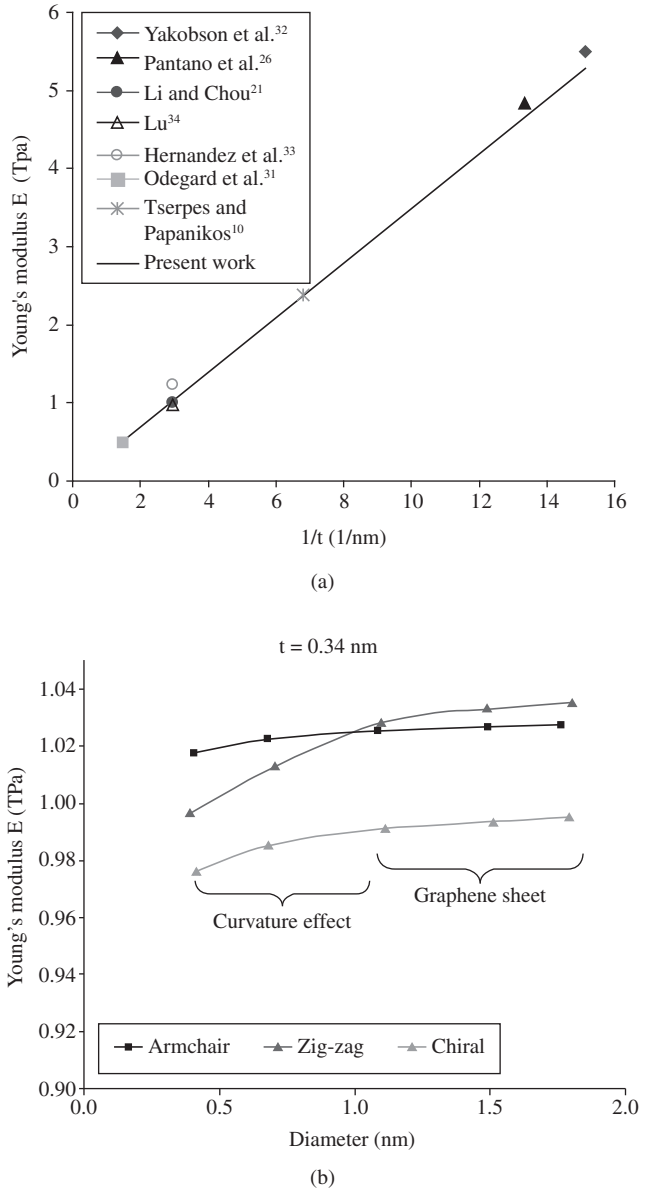

Figure 5. Variation of the Young's Modulus with nanotube diameter for armchair, zigzag and chiral configurations. a) Comparative study; and b) Fixed wall thickness.

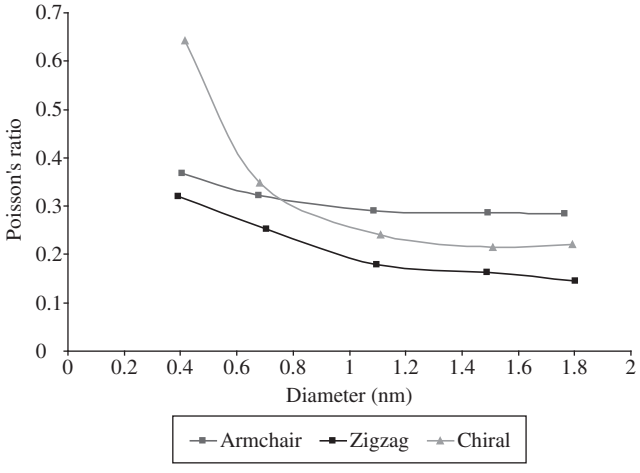

Figure 6. Poisson's ratio variation as a function of nanotube diameter.

From the Poisson ratio variability listed in literature, it is possible to infer that Poisson's ratio can be represented between 0.15 and 0.29. These values are dependent on the nanotube diameter. The results presented by Popov and Van Doren[38] also corroborate the present model findings. Their model based on analytical expression for the velocity of the longitudinal and torsional sound waves in SWNTs leads to an asymptotic value of Poisson's ratio of 0.21. However, one final result has to be analyzed, the Poisson's ratio of 0.64. One possible explanation for such result is the CNTs geometry. This data corresponds to the chiral (4,2) configuration. From Figure 7, it is possible to observe that for this configuration, the transverse section is not hexagonal but pentagonal. This geometry leads to a much larger axial strain which has direct influence into Poisson's ratio.

A final issue that must be analyzed is the RVE selection criterion and its boundary conditions imposition. For a carbon nanotube, the RVE or unit cell is represented by a group of C-C bonds rings. For each carbon nanotube configuration, one unique C-C bond ring is defined. The largest normal stress for the armchair configuration, showed in Figure 8a, is located into the bond angle variation region. Meanwhile, the zigzag format, showed in Figure 8b, has the largest normal stress distribution on dihedral angle torsion region (pointed by the arrows). These finds agree with analytical predictions made by Lu and Zhang[35] who pointed these locations as the ones with highest probability of failure. The stress distribution for the chiral configuration, represented in Figure 8c, is much more complex, where large normal stresses are found in different points along the SWNT length.

When the failure mechanism is analyzed, the normal stress distribution directs us to locus of higher probability of failure. Those regions are the bond angle variation for the armchair configuration, the dihedral angle torsion region for the zigzag case, while the chiral configuration showed different regions of failure probability. Figures 9a-c show the deformed shapes. Notice that for chiral case, the final deformed shape is totally distinct from the two others. The carbon atoms rotation due to chiral angle could be the cause of this complex deformed shape. Still, the imposition of boundary conditions is also affected by this "atom rotation". Note that boundary conditions are affected, and the RVE geometry is also "changed" when the chiral configuration is analyzed, as it can be seen in Figure 9c. A similar behavior during molecular mechanics simulation was also observed by Tserpes and Papanikos[10]. They also pointed out that chirality's was the major issue during SWNT's simulation. Still, chiral configurations can always be reduced to armchair and zigzag formats.

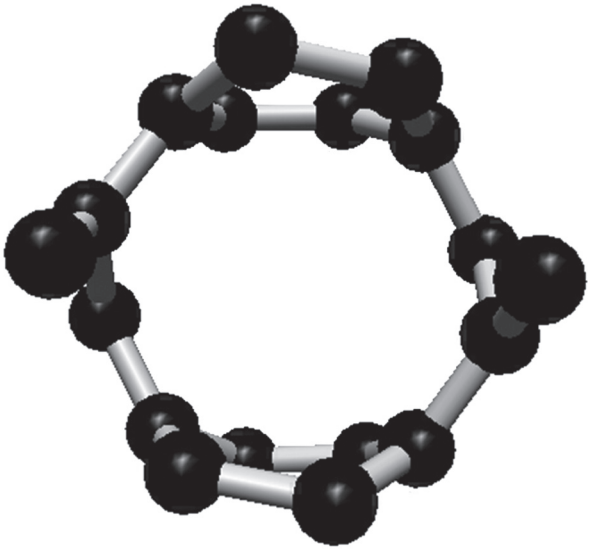

Figure 7. Representative volume element for a chiral (4,2) configuration.

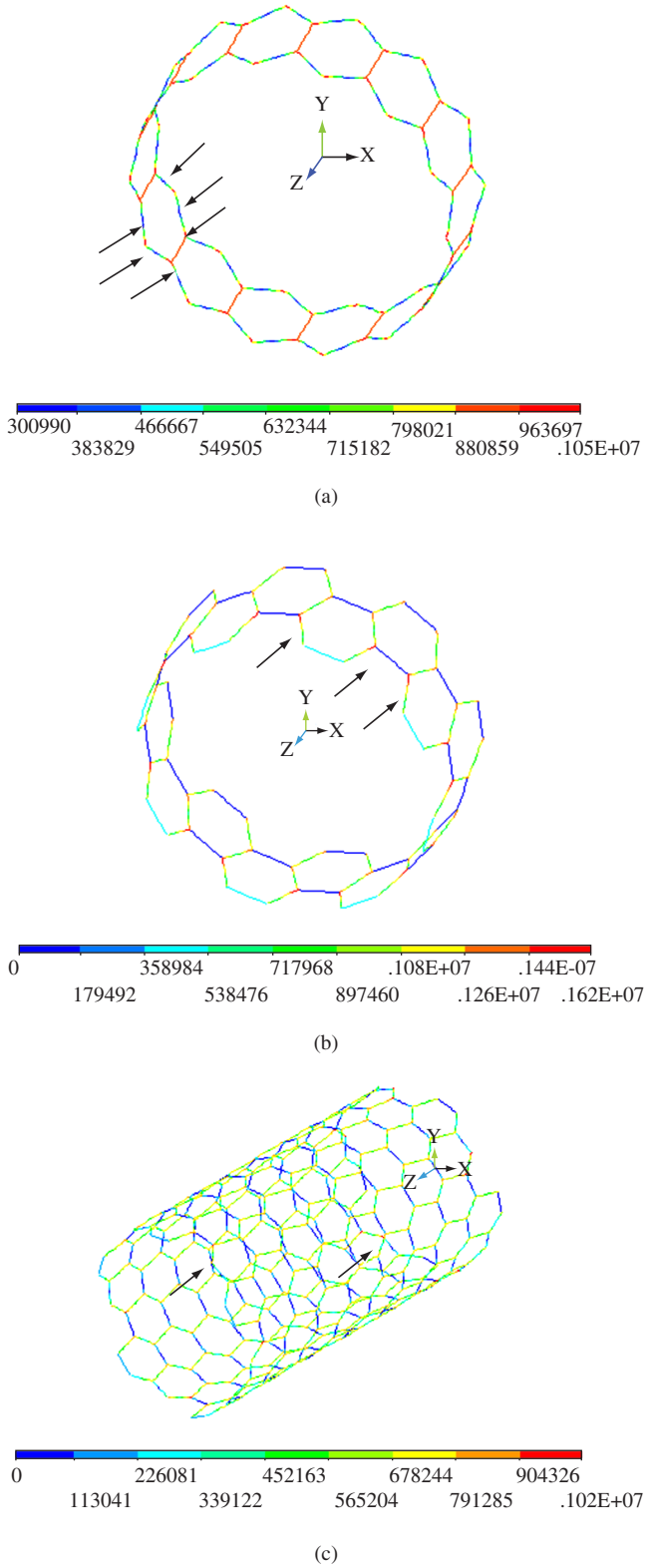

Figure 8. Normal stress distribution on SWNT configurations, a) armchair; b) zigzag; and c) chiral.

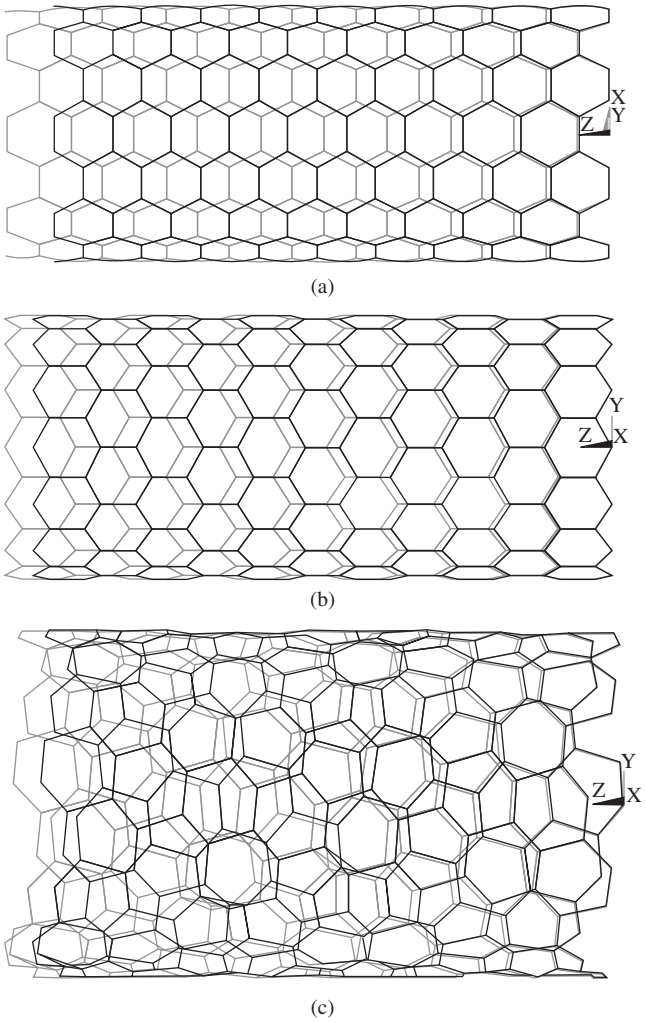

Figure 9. Deformed shape of SWNT: a) (8,8) armchair; b) (14,0) zigzag; and c) (11,5) chiral.

4. Conclusion

A molecular mechanics model for armchair, zigzag and chiral single-walled carbon nanotubes has been implemented. One advantage of such approach is that it's easy implementation and considerably lowers computational efforts when compared against other numerical techniques. The molecular structural mechanics approach was employed to exam the effect of wall thickness, diameter and chirality's effect on SWNT stiffness.

The results suggested that stiffness (Young's modulus) is inversely proportional to wall thickness. Moreover, the curvature effect due to SWNT radius has also an effect on stiffness. Smaller radius conducts to larger curvatures and elongations. Meanwhile, on SWNT with large radius, the curvature effect is negligible and Young's modulus approaches the graphene sheet modulus (≈1.0 TPa).

The SWNT configuration less affected by the radius/curvature variations seems to be the chiral one due to its complex geometry. The SWNT unit cell stress distributions also revealed critical regions where the failure is most likely to occur. For armchair case, it seems to be the bond angle variation region, while for the zigzag case the dihedral angle torsion region is the critical one. The chiral case guide to different locations of high stresses concentration as a function of the atoms location.

The molecular structural mechanics approach is an effective atomistic modeling technique for simulating carbon nanotubes. The Poisson's ratio of SWNT was also simulated and the results were between 0.15-0.29. Notice that nanotube radius variations also affect the Poisson's ratio. Again the chiral configuration seems to be the most sensible to radius variations.

Given this data, this approach seems to be a powerful tool for modeling nanocomposites with accuracy.

Acknowledgements

The authors would like to acknowledge the financial support provided by the Brazilian Research Council (CNPq) under research grants 550067/2005-1, 300826/2005-2 and 470511/2006-0. Additional financial support was provided by the Institute of Nanotechnology (MCT/CNPq) and the Graduate Studies Program in Mechanical Engineering (PPGMEC) of the Universidade Federal de Minas Gerais.

References

1. Iijima S. Helical microtubes of graphitic carbon. *Nature* 1991; 354:56-58.
2. Frankland SJV, Harik VM, Odegard GM, Brenner DW, Gates TS. The stress-strain behavior of polymer–nanotube composites from molecular dynamics simulation. *Composites Science and Technology* 2003; 63(10):1655-1661.
3. Jin Y, Yuan FG. Simulation of elastic properties of single-walled carbon nanotubes. *Composites Science and Technology* 2003; 63(8):1507-1515.
4. Agrawal PM, Sudalayandi BS, Raff LM, Komanduri R. A comparison of different methods of Young's modulus determination for single-wall carbon nanotubes (SWCNT) using molecular dynamics (MD) simulations. *Computational Materials Science* 2006; 38(2):271-281.
5. Belytschko T, Xiao SP, Schats GC, Ruoff RS. Atomistic simulations of nanotube fracture. *Physics Review B* 2002; 65:2354301-2354308.
6. Lurie S, Belov P, Volkov-Bogorodsky D, Tuchkova N. Nanomechanical modeling of the nanostructures and dispersed composites. *Computational Materials Science* 2003; 28(4):529-539.
7. Liu WK, Karpov EG, Zhang S, Park HS. An introduction to computational nanomechanics and materials. *Computer Methods in Applied Mechanics and Engineering* 2004; 193(10):1529-1578.
8. Ruoff RS, Pugno N. Mechanics of Nanostructures. In: TJ Chuang et al. (eds.) *Nanomechanics of Materials and Structure*. Amsterdam: Springer; 2006. p. 199-203.
9. Li C, Chou TW. A structural mechanics approach for the analysis of carbon nanotubes. *International Journal of Solids and Structures* 2003; 40(10):2487-2499.
10. Tserpes KI, Papanikos P. Finite Element modeling of single-walled carbon nanotubes. *Composite: Part B* 2005; 36(4):468-477.
11. Saito R, Dresselhaus G, Dresselhaus MS. Physical Properties of Carbon Nanotubes. Imperial, London: College Press; 2005.
12. Kalamkarov AL, Georgiades AV, Rokkam SK, Veedu VP, Ghasemi-Nejhad MN. Analytical and numerical techniques to predict carbon nanotubes properties. *International Journal of Solids and Structures* 2006; 43(20):6832-6854.
13. Natsuki T, Tantrakarn K, Endo M. Effects of carbon nanotube structures on mechanical properties. *Applied Physics A: Materials Science and Processing* 2004; 79(1):117-124.
14. Yu MF, Lourie O, Dyer MJ, Moloni K, Kelly TF, Ruoff RS. Strength and breaking mechanics of multiwalled carbon nanotubes under tensile load. *Science* 2000; 287(6):637-640.
15. Krishnan A, Dujardin E, Ebbesen TW, Yianilos PN, Treacy MMJ. Young's modulus of single-walled nanotubes. *Physics Review B* 1998; 58(20):4013-4019.

16. Lourie O, Wagner HD. Evaluation of Young's modulus of carbon nanotubes by micro-Raman spectroscopy. *Journal of Materials Research* 1998; 13(20):2418-2422.

17. Xiao JR, Gama BA, Gillespie-Jr. JW. An analytical molecular structural mechanics model for the mechanical properties of carbon nanotubes. *International Journal of Solids and Structures* 2005; 42(24):3075-3092.

18. Dresselhaus MS, Dresselhaus G, Saito R. Physics of carbon nanotubes. *Carbon* 1995; 33(7):883-891.

19. Wang Y, Sun C, Sun X, Hinkley J, Odegard GM, Gates TS. 2-D nano-scale finite element analysis of a polymer field. *Composites Science and Technology* 2003; 63(10):1581-1590.

20. Liu WK, Park HS, Qian D, Karpov EG, Kadowaki H, Wagner GJ. Bridging scale methods for nanomechanics and materials. *Computer Methods and Applied Mechanics in Engineering* 2006 195(12):1407-1421.

21. Li C, Chou TW. Modeling Carbon Nanotubes in their Composites. TJ Chuang, et al. (editors). *Nanomechanics of Materials and Structures*. Amsterdam: Springer; 2006. p. 55-65.

22. Zienkiewicz OC, Taylor RL. *The Finite Element Method*. New York: McGraw-Hill; 1989.

23. Meo M, Rossi M. Prediction of Young's modulus of single wall carbon nanotubes by molecular-mechanics based finite element method. *Composites Science and Technology* 2006; 66(10):1597-1605.

24. Koloczek J, Kwon YK, Burian A. Characterization of spatial correlations in carbon nanotubes-modeling studies. *Journal of Alloys and Compounds* 2001; 328(2):222-225.

25. Sun X, Zhao W. Prediction of stiffness and strength of single-walled carbon nanotubes by molecular-mechanics based finite element approach. *Materials Science and Engineering A* 2005; 390(3):366-371.

26. Pantano A, Parks DM, Boyce MC. Mechanics of deformation of single- and multi-wall carbon nanotubes. *Journal of the Mechanics and Physics of Solids* 2004; 52(6):789-821.

27. Huang MY, Chen HB, Lu JN, Zhang PQ. A modified molecular structural mechanics method for analysis of carbon nanotubes. *Chinese Journal of Chemical Physics* 2006; 19(4):286-290.

28. Ávila AF, Lacerda GSR. From nano to macromechanics: A molecular mechanics analysis of single-walled carbon nanotubes. *Proceedings of the 19th International Congress of Mechanical Engineering* [CD-ROM]; 2007 Nov 5-9; Brasília, Brazil: Universidade de Brasilia; 2007.

29. Tamma KK, Ávila AF. An Integrated Micro/Macro Modeling and Computational Methodology for High Temperature Composites. Thermal Stress. V, Richard-Hetnarski (eds.). Honeoeye Falls: Lastran Corporation; 1999. p. 143-256.

30. Ávila AF, Lacerda GSR. *A Molecular Structural Mechanics Investigation on Single Walled Carbon Nanotubes*. Book of Abstracts of the 8th International Congress of Carbon Nanotubes, Ouro Preto; 2007.

31. Odegard GM, Gates TS, Nicholson LM, Wise KE. Equivalent continuum modeling of nano-structured materials. *Composites Science and Technology* 2002; 62(10):1869-1880.

32. Yakobson BI, Brabec CJ, Bernholc J. Nanomechanics of carbon tubes: instabilities beyond linear range. *Physical Review Letters* 1996; 76(20):2511-2514.

33. Hernandez E, Goze C, Bernier P, Rubio A. Elastic properties of C and BxCyNz composite nanotubes. *Physical Review Letters* 1998; 80(20):4502-4505.

34. Lu JP. Elastic properties of carbon nanotubes and nanoropes. *Physical Review Letters* 1997; 79(7):1297-300.

35. Lu J, Zhang L. Analysis of localized failure of single-wall carbon nanotubes. *Computational Materials Science* 2006; 35(3):432-441.

36. Ávila AF, Duarte HV, Soares MI. The Nanoclay Influence on Impact Response of Laminate Plates. *Latin American Journal of Solids and Structures* 2006; 3(1):1-20.

37. Salvetat-Delmont JP, Rubio A. Mechanical properties of carbon nanotubes: a fiber digest for beginners. *Carbon* 2002; 40(10):1729-1734.

38. Popov VN, Van Doren VE. Elastic Properties of single-walled carbon nanotubes. *Physical Review B* 2000; 61(4):3078-3084.